ISSN 0020-1685, Inorganic Materials, 2014, Vol. 50, No. 1, pp. 75–81. © Pleiades Publishing, Ltd., 2014.
Original Russian Text © L.A. Zemnukhova, A.E. Panasenko, E.A. Tsoi, G.A. Fedorishcheva, N.P. Shapkin, A.P. Artem'yanov, V.Yu. Maiorov, 2014, published in Neorganicheskie Materialy, 2014, Vol. 50, No. 1, pp. 82–89.

Composition and Structure of Amorphous Silica Produced from Rice Husk and Straw

L. A. Zemnukhova[a, b], A. E. Panasenko[a], E. A. Tsoi[b], G. A. Fedorishcheva[a], N. P. Shapkin[b], A. P. Artem'yanov[b], and V. Yu. Maiorov[a]

[a] *Institute of Chemistry, Far East Branch, Russian Academy of Sciences, pr. Stoletiya Vladivostoka 159, Vladivostok, 690022 Russia*

[b] *Far East Federal University, ul. Sukhanova 8, Vladivostok, 690950 Russia*

e-mail: laz@ich.dvo.ru

Received January 15, 2013

Abstract—We have studied amorphous silica samples prepared by a thermal method and precipitation from rice processing waste: straw and grain shells (husk and peelings). We have determined their true and bulk densities, silica content, and sorbed water vapor content. The porosity of the samples has been evaluated by different techniques: nitrogen desorption (Barrett–Joyner–Halenda method) and adsorption (BET analysis), water vapor adsorption, sorption of organic dyes (methylene blue and brilliant green), and positron annihilation spectroscopy. The effect of the nature of raw materials and processing procedure on the physicochemical properties of amorphous silica is examined.

DOI: 10.1134/S0020168514010208

INTRODUCTION

A priority issue in modern industry is to enable processing of sustainable plant raw materials, including immense amounts of agro waste from annual plants. The main advantages of such raw materials are annual reproducibility, low cost, and an essentially constant chemical composition of a given plant species. In particular, promising raw materials for amorphous silicon dioxide (silica) production are immense amounts of rice processing waste. This has been clearly demonstrated by research groups from various countries and has been the subject of several reviews [1, 2]. However, the physicochemical properties of noncrystalline SiO_2 phases of biogenic origin have not yet been studied in sufficient detail, which probably also inhibits the development of environmentally safe and economically viable processes for extracting silica from plant raw materials.

As part of our studies concerned with the properties of amorphous silica of various origins [3–6], this work focuses on the physicochemical parameters (silica content, sorbed water content, density, and porosity characteristics) of materials prepared from rice husk (RH) and rice straw (RS) through heat treatment and precipitation.

EXPERIMENTAL

Amorphous silica samples (Table 1, samples 1–15) were prepared from RH (Dal'nevostochnyi variety) and RS (Khankaiskii 429, Priozernyi 61, Darii 23, Darii 8, Rassvet, Dolinnyi, Lugovoi, Khankaiskii 52). The plant raw materials were collected in 2010 in settlement Timiryazevskii, Primorskii krai. The husk was sieved, and particles no less than 2 mm in size were used in our experiments. The straw was cut into parts 10–50 mm in length. The materials were washed with water and dried in air. Silica samples were prepared by procedures described previously [6].

Procedure 1. A weighed sample was first charred at 300°C to remove volatiles and then fired in a muffle in air (or thermolysis was performed, procedure 1*) at 600–700°C to constant weight.

Procedure 2. A weighed sample was treated with a 0.1 N hydrochloric acid solution at 90°C for 1 h and then filtered off. The filtrate was washed with water, dried, and then charred and fired in a muffle as in procedure 1.

Procedure 3. A weighed sample was treated with a 1 N potassium or sodium hydroxide solution at 90°C for 1 h. The residual raw material was separated from the solution, and then silica was precipitated by concentrated hydrochloric acid. The precipitate was washed with water until free of sodium or potassium chloride and dried in air at 60°C.

For comparison, we also examined commercially available silica of mineral origin (sample 16): aqueous silicic acid, $SiO_2 \cdot nH_2O$ (RF State Standard GOST 4214-78).

The materials prepared by these procedures (Table 1, samples 1–16) were identified by chemical analysis, IR spectroscopy (Shimadzu FTIR Prestige-21 Fourier transform spectrophotometer, frequency range 400–4000 cm^{-1}, Vaseline mulls), X-ray

Table 1. Chemical composition and density of SiO_2 samples prepared from different rice varieties and parts (RH and RS) with preliminary processing by procedures 1–3

No.	Rice variety	Raw material, processing	Silica yield from raw materials η, %	Percent		SiO_2 density	
				SiO_2	H_2O	true, g/cm^3	bulk, g/L
1	Dal'nevostochnyi	RH-1, procedure 2	18.3	99.4	<0.5	2.03	459
2		RH-1, procedure 3	11.0	88.4	7.8	2.00	421
3		RH, procedure 1*	40.0	47.5	<0.5	2.01	457
4	Khankaiskii 429	RS-1, procedure 2	13.5	91.9	<0.1	2.14	570
5	Priozernyi 61	RS-2, procedure 2	12.5	91.6	<0.1	2.12	542
6	Darii 23	RS-3, procedure 2	11.5	91.9	<0.1	2.06	505
7	Rassvet	RS-4, procedure 1	15.0	88.0	<0.1	2.10	562
8		RS-4, procedure 2	13.5	86.9	<0.1	2.19	604
9		RS-4, procedure 3	8.7	91.0	8.9	2.00	420
10	Dolinnyi	RS-5, procedure 1	17.0	87.5	<0.1	2.10	570
11		RS-5, procedure 2	13.5	92.1	<0.1	2.07	487
12		RS-5, procedure 3	5.1	91.0	8.9	2.00	420
13	Lugovoi	RS-6, procedure 2	11.5	93.6	<0.1	2.10	531
14	Khankaiskii 52	RS-7, procedure 2	13.5	90.9	<0.1	2.16	542
15	Darii 8	RS-8, procedure 2	12.3	97.5	<0.1	2.02	500
16	$SiO_2 \cdot nH_2O$, GOST 4214-78			88.4	11.6	2.15	663

Notes: Sample 1 corresponds to amorphous silicon dioxide (ASD) as specified in the Purity Standard TU 2169-276-00209792-2005. Sample 3 corresponds to the TShR silicon–carbon sorbent as specified in the Purity Standard TU 2164-011-02698192-2006 and was prepared through thermolysis of rice husk at 750°C (procedure 1*).

diffraction (Bruker D8 ADVANCE diffractometer, CuK_α radiation), and thermogravimetry (*Q*-1000 thermoanalytical system, air, heating rate of 5 K/min) using standard techniques like in a previous study [6].

The morphology of the samples was examined by high-resolution scanning electron microscopy (SEM) on a Hitachi S 5500.

The true density of the samples was determined in toluene by the Archimedes method at 25°C, and their bulk density was evaluated from measurements of their mass and dimensions by standard techniques.

The specific surface area (*S*) and pore size distribution were determined by nitrogen adsorption measurements with an ASAP 2020 analyzer (Micromeritics Instrument Co.). The values of *S* were obtained by Brunauer–Emmett–Teller (BET) analysis of nitrogen adsorption isotherms, and the pore size distribution was obtained by the Barrett–Joyner–Halenda (BJH) method.

In addition, the specific surface area of the silica samples was determined by water vapor adsorption measurements under isopiestic conditions at 25°C. To this end, dried samples were placed in a thermostated system with controlled water vapor pressure and held their until equilibration (24 h). *S* was evaluated for the capillary condensation region by determining the specific surface area of the adsorbed water film, which was assumed to be equal to the specific surface area of the sample [7]. The effective pore diameter in the samples was determined from the differential pore volume–size distributions derived from water vapor adsorption–desorption isotherms as described elsewhere [8].

The adsorption activity of the samples was characterized by their adsorption capacity for two organic dyes: methylene blue (MB, basic thiazine dye with the formula $C_{16}H_{24}ClN_3O_3S$) and aniline dye brilliant green (BG, aniline dye with the chemical formula $C_{27}H_{34}N_2O_4S$). Sorption of the dyes was conducted by a static method in aqueous solutions with a concentration of 100 mg/L. Isotherms were constructed as plots of $1/\Gamma$ against $1/C$ (where Γ is adsorption and *C* is the equilibrium concentration). The maximum adsorption value Γ_0 was found using the Langmuir equation [9]:

$$\frac{1}{\Gamma} = \frac{1}{\Gamma_0} + \frac{b}{\Gamma_0}\frac{1}{C}.$$

In addition, to determine the size of intracrystalline regions in the amorphous silica samples we used positron annihilation spectroscopy (PAS), which

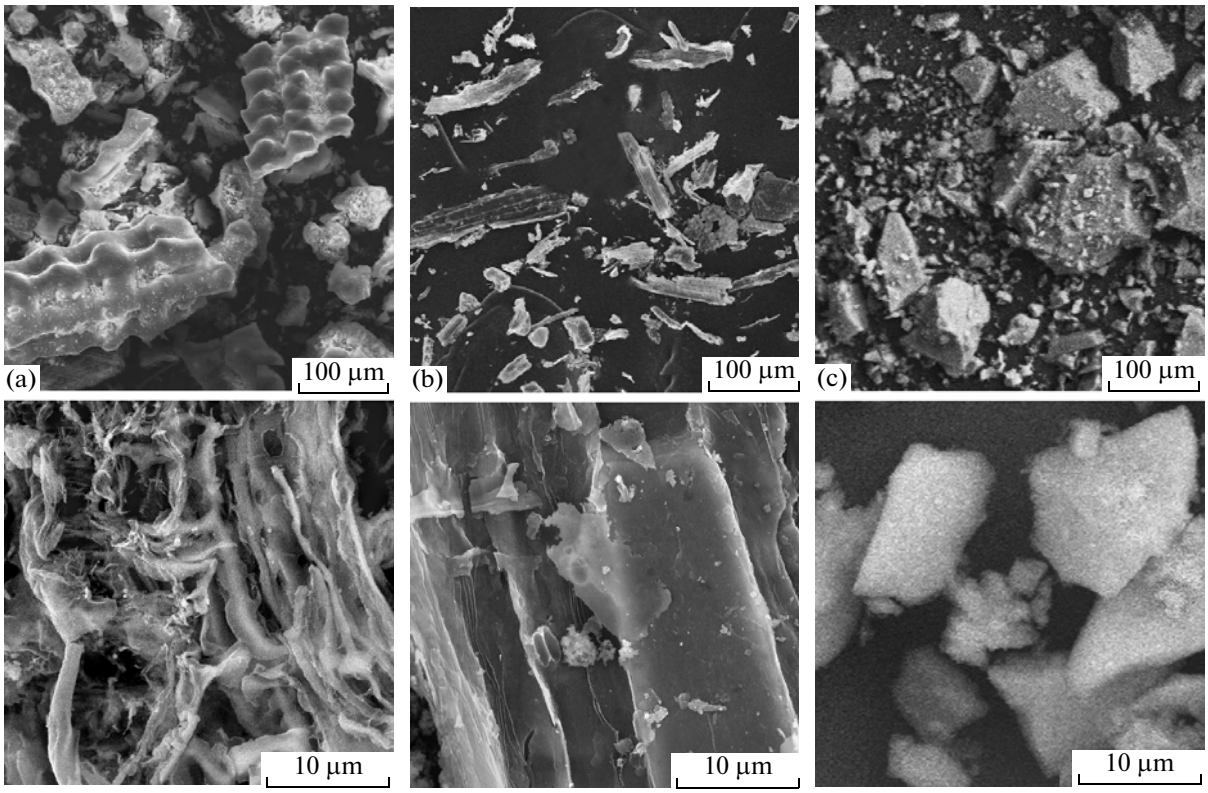

Fig. 1. Micrographs of amorphous silica samples prepared by procedure 2 from (a) RH (sample 1) and (b) RS (sample 11) and by procedure 3 from (c) RH (sample 2).

involves positron lifetime measurements [10]. Spectra were taken using a fast–fast delayed coincidence scintillation spectrometer based on a Nokia-LP-4840 multichannel analyzer and FEU-87 photomultiplier [11]. The time resolution of the spectrometer $2\tau_0$ was 270 ns for a ^{60}Co source at an energy window of 30%. In lifetime measurements, we used a ^{44}Ti cyclotron positron source with an activity of 10–15 mCi.

RESULTS AND DISCUSSION

Below, we present results on the properties of amorphous silica samples prepared from rice husk and straw by different procedures (Table 1).

Composition and density of the samples. X-ray diffraction examination showed that all of the silica samples obtained (Table 1) were X-ray amorphous: their X-ray diffraction patterns were typical of amorphous materials, like in previous studies [3, 4, 6]. In procedures 1–3, the silica yield η was 9–17% relative to the raw materials and depended primarily on the processing procedure. It is worth pointing out, however, that, for a given procedure, the silica yield from RH was, as a rule, 2–4% higher than that from RS [6]. The SiO_2 and sorbed water contents of products obtained from the same raw material are also determined by the processing procedure. In particular, in the products obtained from RH (Table 1, samples 1–3) the silica content was 47.5, 88.4, and 99.4% and the water content ranged from ≃0.5 to 7.8%. The products extracted from rice straw (samples 4–6, 8, 11, 13–15) contained less SiO_2 in comparison with husk. The amorphous silica samples prepared from RS by procedures 1 and 2 sorbed negligible amounts of water, in contrast to their analogs prepared from RH (Table 1). The water content of the samples prepared by procedure 3 from alkaline hydrolysis's of the raw materials (both RH and RS) was considerably higher (≃8–9%) than that of the samples obtained by procedures 1 and 2. In sample 16 (reference), the sorbed water content was 11.6%.

Density and morphology. It is seen from Table 1 that all of the samples differ little in true density (2.00–2.19 g/cm^3), whereas their bulk densities differ by more than a factor of 1.5 (from 420 to 663 g/L). The bulk density of the samples prepared by procedure 2 from RH (459 g/L) is lower than that of the samples obtained from RS (487–604 g/L). The scatter suggests that the structure of amorphous silica depends on the processing procedure, the type of waste (husk or straw), and the rice variety.

Figure 1 presents micrographs of the SiO_2 samples prepared by procedure 2 from RH (Fig. 1a, sample 1) and RS (Fig. 1b, sample 11) and by procedure 3 from RH (Fig. 1c, sample 2). It is seen that, in the case of acid hydrolysis of the raw materials, followed by calcination (Figs. 1a, 1b), the silica to some extent retains

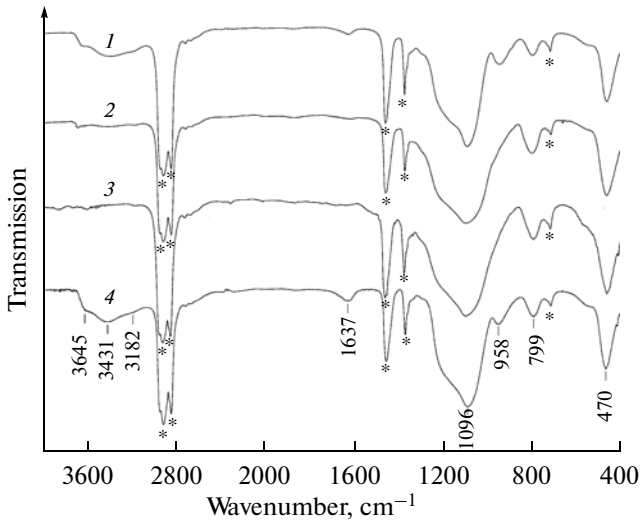

Fig. 2. IR absorption spectra of amorphous silica: samples (*1*) 16, (*2*) 1, (*3*) 8, and (*4*) 12. Asterisks mark the absorption bands of Vaseline oil.

the structure of plant tissue. The sample prepared from RH consists of particles up to 300 μm in size, and their surface replicates the surface topography of the grain shell. Examination of fracture surfaces of such particles at a high magnification demonstrates that their bulk is not monolithic but consists of thin porous structures with elements 1 mm and less in thickness (Fig. 1a). By contrast, the silica sample prepared from RS consists of finer particles (10 to 150 μm in size), which typically have a dense structure with insignificant porosity (Fig. 1b). The silica sample prepared through precipitation from an alkaline solution (Fig. 1c) consists of irregular, acute-angled particles which range in size from 200 to 1 μm or even less. It seems likely that the particles in this sample are not monolithic but have a highly porous structure, which is supported by its low bulk density.

IR absorption spectra. Figure 2 shows typical IR absorption spectra of the amorphous silica samples (samples 1, 8, 12) prepared from rice husk (spectrum *2*) and straw (spectrum *3*) by procedure 2 and by precipitation from an alkaline hydrolyzate of the raw materials by procedure *3* (spectrum *4*). Also presented for comparison is the spectrum of commercially available silica, sample 16 (spectrum *1*). All of the spectra contain absorption bands near 470, 799, and 1100 cm^{-1}, corresponding to stretching and bending modes of the Si–O–Si siloxane bonds present in amorphous silica according to previous studies [12]. In addition, the spectra of the samples prepared from RH by procedure 2 (spectrum *2*) contain weak bands characteristic of stretching (3182, 3400, and 3694 cm^{-1}) and bending (1624 cm^{-1}) vibrations of O–H bonds and sorbed water molecules. The feature at 958 cm^{-1} is due to a small concentration of Si–OH silanol bonds. The spectra of the samples prepared by procedure 2 from RS (spectrum *3*) contain no such absorptions. The IR spectra of the silica samples prepared from rice husk and straw by procedure 3 (spectrum *4*) differ from the above spectra in that they contain a medium strong band at 958 cm^{-1}, which clearly indicates the presence of Si–OH silanol bonds, and stronger bands at 3182, 3431, 3645, and 1637 cm^{-1}, due to O–H bonds. Sample 16 has a similar spectrum (spectrum *1*). Analysis of the IR absorption spectra of the samples correlates with sorbed water content (Table 1). Thus, samples 2, 9, 12, and 16 contain more Si–OH silanol bonds than do samples 1 and 3, and samples 4–8, 10, 11, and 13–15 contain negligible concentrations of silanol bonds.

Specific surface area, pore diameter, and sorption capacity. Table 2 characterizes the porosity of the silica samples. The specific surface areas evaluated by BET analysis of nitrogen adsorption data demonstrate that the samples prepared from RH (samples 1–3) have the highest S values, in the range 230–479 m^2/g, depending on the preparation procedure. The high S values of samples 1 and 2 correlate with their microstructures in micrographs (Figs. 1a, 1c). The SiO_2 samples prepared from RS by procedure 2 have lower S values (8.6–102 m^2/g), which illustrates the effect of rice variety on the porosity of the silica present in the structure of the straw.

The average pore diameters and pore size distributions evaluated from nitrogen adsorption data (BET) are presented in Table 2 and Fig. 3. In the silicas prepared from RH (samples 1–3), the predominant pore diameters are 3.9–4.4 nm. The precipitated silica (sample 2) contains smaller pores. Therefore, these samples have a predominantly mesoporous structure. The average pore diameter in the SiO_2 samples prepared from RS ranges more widely, from 9.9 to 85.7 nm, indicating the presence of both mesopores (samples 5, 6, 12–14) and macropores (samples 4, 8).

Data on the pore structure of some of the samples as evaluated from water vapor adsorption data are also presented in Table 2. This method allows one to assess mainly hydrophilic surfaces, so the specific surface areas obtained characterize the sorption capacity of the samples for extraction of components from aqueous solutions. It is worth pointing out that sample 3 was poorly wetted by water, in contrast to the other samples. It seems likely that it had a hydrophobic surface. The hydrophobic properties of surfaces play a key role in water sorption processes, so the average pore diameters evaluated from nitrogen and water vapor sorption data for hydrophobic samples may differ markedly, as observed in the present experimental data (samples 3, 5, 13).

The marked discrepancy between the specific surface areas evaluated from nitrogen and water vapor sorption data for samples 1, 3, 5, and 11 originates from the fact that the samples differ in the amount of micropores according to water vapor desorption data. Calculation results for micropores are very sensitive to the size of adsorbate molecules used to study the pore

Table 2. Structural characteristics and sorption capacity of SiO_2 as evaluated from nitrogen physisorption, water vapor adsorption, organic dye (BG and MB) adsorption, and PAS data

No.	Nitrogen physisorption		Water vapor adsorption		Sorption capacity for organic dyes, mg/g		Average volume of positronium "traps" according to PAS data, V_{tr}, Å^3
	S, m^2/g	average pore diameter, nm	S, m^2/g	average pore diameter, nm	BG	MB	
1	230.8	4.4	53.4	5.6	83.7	68.3	258
2	479.0	3.9					
3	260.1	4.2	43.5	1.94	33.3		161.8
4	11.0	52.7			61.8	117.1	94.7
5	34.9	19.2	75.5	6.5		162.3	
6	46.7	9.9			90.8	169.0	93.5
8	8.6	85.7				145.0	
11	31.0		74.6	6.4	126.5	191.8	107.9
12	30.6	20.1					51.6
13	33.0	19.6	21.5	2.8	112.2	170.6	98.1
14	26.2	33.5			72.3	168.2	103.9
15	102.4	6.9					
16	73.0		80.5	1.6	30.0	124.9	154.2

structure of the samples. The satisfactory agreement between the S values obtained by the two methods for samples 13 and 16 points to a more homogeneous structure of the silica: predominantly mesoporous (sample 13) and microporous (sample 16). Clearly, the sample surface in this case is hydrophilic and accessible for both nitrogen and water molecules.

The sorption capacity of silicon-containing sorbents for organic dyes, including BG and MB, has been the subject of extensive studies [13]. The sorption capacities (Γ_0) of our amorphous silica samples for BG and MB are indicated in Table 2. The values for sample 1 (prepared from RH) differ little (Table 2), whereas the samples prepared from RS (4, 6, 11, 13, 14) have different sorption capacities for these dyes. At the same time, the sorption capacity for MB is about a factor of 1.5 higher than that for BG. This distinction is attributable to the higher basicity of MB, whose molecule contains three nitrogen atoms and has conjugation between two benzene rings through nitrogen and sulfur atoms. It seems likely that each molecule of these substances (BG and MB) has its own active centers, which are involved in the interaction with the sorbent surface. For example, as shown by Ovchinnikov et al. [14], when MB interacts with a AgCl surface, the most active species are the unsaturated dimethylamino groups and the sulfur atom in the heterocycle of this dye, which can participate in the formation of hydrogen bonds with the sorbent surface. Comparison of the sorption capacities for BG and MB (Table 2) with IR spectroscopy data (Fig. 2) indicates that the presence and density of siloxane (Si–OH) bonds on the surface of amorphous silica play no significant role. Moreover, the sorption capacities of sample 16 (which contains siloxane bonds as evidenced by the medium strong IR absorption band at 958 cm^{-1}) for BG and MB are lower than those of the samples prepared from RS (samples 4–6, 8, 11, 13, 14), which contain no such bonds.

Positron annihilation spectroscopy. One important physicochemical characteristic of sorbents is the presence and size of internal defects, which play an important role in determining the sorption of particular sub-

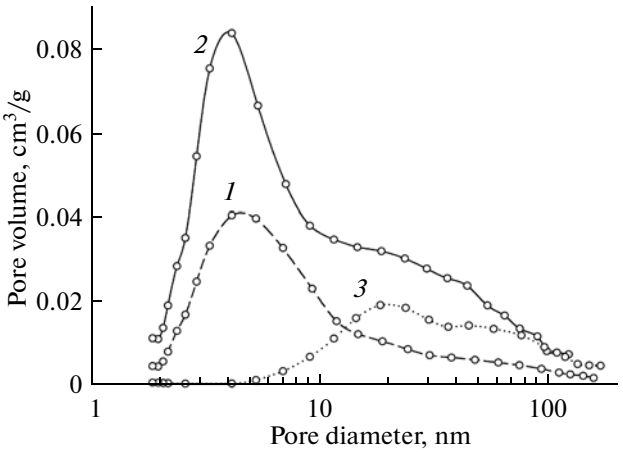

Fig. 3. Pore size distributions extracted from nitrogen adsorption data for amorphous silica samples prepared by procedure 2 from (*1*) rice husk (sample 1) and (*3*) rice straw (sample 4) and by procedure 3 from (*2*) rice husk (sample 2).

Table 3. Experimentally determined and calculated parameters derived from PAS data for the amorphous silica samples

No.	Experimental data						Calculation results								
	τ_1, $s \times 10^{-9}$	I_1, %	τ_2, $s \times 10^{-9}$	I_2, %	τ_3, $s \times 10^{-9}$	I_3, %	ν_{ps}, $s^{-1} \times 10^8$	ν_{e+}, $s^{-1} \times 10^8$	N_{ps}, $cm^{-3} \times 10^{21}$	N_{e+}, $cm^{-3} \times 10^{21}$	R_{ps}, Å	R_{e+}, Å	V_{ps}, arb. units	V_{e+}, arb. units	V_{tr}, Å^3
1	0.141	60.8	0.345	31.2	2.396	8.0	1.79	9.32	1.01	7.12	5.87	4.34	8.604	24.376	258.0
3	0.153	70.5	0.362	27.1	0.573	2.4	1.19	7.36	0.89	5.63	4.43	4.34	3.246	19.258	161.8
4	0.131	59.4	0.302	31.8	1.075	8.8	7.41	10.78	4.97	8.22	4.94	4.34	2.511	2.852	94.7
6	0.154	58.9	0.304	29.9	0.869	11.1	7.85	7.85	5.64	5.95	4.61	4.38	23.218	20.892	93.5
11	0.160	63.3	0.291	25.2	0.904	11.5	7.72	5.84	5.52	4.41	4.63	4.39	22.995	15.639	107.9
12	0.112	42.6	0.284	47.3	0.936	10.1	12.1	19.8	8.28	15.0	4.83	4.36	3.910	5.239	51.6
13	0.153	60.0	0.311	29.4	0.950	10.6	4.55	7.89	5.34	5.99	4.69	4.37	23.042	20.911	98.1
14	0.149	61.2	0.317	29.3	1.011	9.6	6.93	8.27	4.82	6.30	4.77	4.36	21.885	21.799	103.9
16	0.173	64.4	0.314	27.2	1.388	8.4	5.34	5.43	3.59	4.10	4.93	4.39	17.998	14.550	154.2

Note: τ_1 is the positron or positronium lifetime, τ_2 is the lifetime of the short-lived component, τ_3 is the lifetime of the long-lived component, I_1 is the intensity of the first component, I_2 is the intensity of the short-lived component, I_3 is the intensity of the long-lived component, ν_{ps} is the rate of the interaction between a positronium and the medium, ν_{e+} is the rate of the interaction between a positron and the medium, N_{ps} is the concentration of positronium traps, N_{e+} is the concentration of positron traps, R_{ps} is the positronium trap radius, R_{e+} is the positron trap radius, V_{ps} is the free volume of structurally disordered regions, V_{e+} is the free volume of structurally ordered regions, and V_{tr} is the average trap volume.

stances. We took advantage of positron annihilation spectroscopy (PAS) [10], which was successfully used previously to investigate physicochemical characteristics of zeolites [15].

Table 3 presents experimentally determined and calculated parameters derived from PAS data for the amorphous silica samples. Experimental data are commonly interpreted using a model of positronium "traps" in a condensed medium [10]. Solutions to rate equations for positron capture are used to evaluate trap parameters. This is possible because positron lifetimes at defects are functions of the effective defect size. Since positron lifetime distribution spectra can be decomposed into components having both a positron nature and a positronium nature, PAS provides information about the concentration and dimensions of free volume elements in regions differing in the degree of order.

Analysis of the data presented in Table 3 allows us to divide the amorphous SiO_2 samples into two groups. In the samples prepared from rice husk (samples 1, 3), the trap concentration N_{ps} is a factor of 4–5 lower than that in the samples prepared from rice straw (samples 4, 6, 11–14), like in sample 16. In addition, the trap volume (V_{tr}) in the former group is almost twice that in the latter. The large volumes of positronium traps in samples 1, 3, 11, 14, and 16 indicate the presence of micropores in their structure, which is consistent with the nitrogen and water vapor sorption data. The pore structure of the amorphous silica samples prepared from rice husk and straw by different procedures is nonuniform, and the samples differ in defect density, as evidenced by the different volumes of the structurally ordered and disordered regions (Table 3).

CONCLUSIONS

We have prepared amorphous silica samples from rice husk and straw, which can be used in various industrial applications as both silicon–carbon materials and purer forms of silica. The silica yield (5–40%), SiO_2 content (47 to 99+%), and the sorbed water content (<0.1–8.9%) are determined by the nature of the raw materials (straw or husk) and processing conditions. The true density of the samples lies in the range 2.00–2.19 g/cm^3, and their bulk density ranges widely, from 420 to 604 g/L. We have determined the BET surface area of the samples from nitrogen (8.6–479.0 m^2/g) and water vapor (21.5–75.5 m^2/g) adsorption measurements and their sorption capacities for two organic dyes: methylene blue (68.3–191.8 mg/g) and brilliant green (33.3–126.5 mg/g). Data have been obtained on the pore size distribution: the samples contain predominantly mesopores; macro- and micropores are less abundant. Positron annihilation spectroscopy has been used to assess the density of various defects in the pore structure of the amorphous silica samples prepared from rice processing waste.

REFERENCES

1. Govindarao Venneti, M.N., Utilization of rice husk—a preliminary analysis, *J. Sci. Ind. Res.*, 1980, vol. 39, no. 9, p. 495.
2. Sergienko, V.I., Zemnukhova, L.A., Egorov, A.G., et al., Sustainable sources of chemical raw materials: Combined processing of rice and buckwheat production waste, *Ross. Khim. Zh.*, 2004, vol. 48, no. 3, p. 116.
3. Zemnukhova, L.A., Babushkina, T.A., Ziatdinov, A.M., et al., Impurity paramagnetic Fe(III) and Mn(II) centers in samples of amorphous silica of different origin, *Russ. J. Appl. Chem.*, 2012, vol. 85, no. 7, p. 1011.
4. Zemnukhova, L.A., Babushkina, T.A., Klimova, T.P., et al., Structural features of amorphous silica from plants, *Appl. Magn. Reson.*, 2012, vol. 42, no. 4, p. 557.
5. Zemnukhova, L.A., Fedorishcheva, G.A., Shkorina, E.D., et al., Amorphous silicon dioxide from waste of ferroalloy production, *Russ. J. Appl. Chem.*, 2011, vol. 84, no. 4, pp. 565.
6. Zemnukhova, L.A., Egorov, A.G., Fedorishcheva, G.A., et al., Properties of amorphous silica produced from rice and oat processing waste, *Inorg. Mater.*, 2006, vol. 42, no. 1, p. 24.
7. Gregg, S.J. and Sing, K.S.W., *Adsorption, Surface Area, and Porosity*, New York: Academic, 1982.
8. Dubinin, M.M., Water vapor adsorption and microporous structures of carbon adsorbents, *Izv. Akad. Nauk SSS, Ser. Khim.*, 1981, no. 1, p. 9.
9. Zakharchenko, V.N., *Kolloidnaya khimiya* (Colloid Chemistry), Moscow: Vysshaya Shkola, 1974.
10. Grafutin, V.I. and Prokop'ev, E.P., Application of positron annihilation spectroscopy in structural studies, *Usp. Fiz. Nauk*, 2002, vol. 172, no. 1, p. 67.
11. Belyaev, V.N., Kovalen', V.Yu., Razov, V.I., et al., System for positron and positronium lifetime measurements in condensed media, *Prib. Tekh. Eksp.*, 1980, no. 6, p. 47.
12. *Infrakrasnye spektry neorganicheskikh stekol i kristallov* (Inorganic Spectra of Inorganic Glasses and Crystals), Vlasov, A.G. and Florinskaya, V.A., Eds., Leningrad: Khimiya, 1972.
13. Ahmaruzzaman, M. and Gupta, V.K., Rice husk and its ash as low-cost adsorbents in water and wastewater treatment, *Ind. Eng. Chem. Res.*, 2011, vol. 50, p. 13589.
14. Ovchinnikov, O.V., Chernykh, S.V., Smirnov, M.S., et al., Interaction of methylene blue with the surface of AgCl(I) microcrystals, *Zh. Prikl. Spektrosk.*, 2007, vol. 74, no. 6, p. 731.
15. Mashkova, S.A., Razov, V.I., Tonkikh, I.V., et al., Preparation and adsorption properties of modified natural sorbents, *Izv. Vyssh. Uchebn. Zaved., Khim. Khim. Tekhnol.*, 2005, vol. 48, no. 5, p. 112.

Translated by O. Tsarev